Model ecosystem with variable interspecies interactions

2007 J. Phys. A: Math. Theor. 40 8723

(http://iopscience.iop.org/1751-8121/40/30/008)

IOP PUBLISHING JOURNAL OF PHYSICS A: MATHEMATICAL AND THEORETICAL

J. Phys. A: Math. Theor. **40** (2007) 8723–8738 doi:10.1088/1751-8113/40/30/008

Model ecosystem with variable interspecies interactions

Fábio C Poderoso and José F Fontanari

Instituto de Física de São Carlos, Universidade de São Paulo, Caixa Postal 369, 13560-970 São Carlos SP, Brazil

Received 13 March 2007, in final form 7 June 2007
Published 12 July 2007
Online at stacks.iop.org/JPhysA/40/8723

Abstract

Model ecosystems with quenched, symmetric interspecies interactions have been extensively studied using the replica method of the statistical mechanics of disordered systems. Here, we consider a more general scenario in which both the species abundances and the interspecies interactions change with time, albeit in widely separated timescales. The equilibrium of the coupled dynamics is studied analytically within the partial annealing framework, in which the number of replicas n takes on positive as well as negative values. In the case $n > 0$, which describes ecosystems characterized by the cooperative interspecies interactions, we find a discontinuous transition to a regime of zero diversity, whereas in the case where competition prevails, $n < 0$, we find that the species diversity is maximum.

PACS numbers: 87.23.Cc, 75.10.Nr

1. Introduction

An interesting though rarely pointed out parallel between the physics of disordered systems and the organization of ecosystems is the existence of two widely separated timescales for the evolution of the relevant variables that describe those systems. In physics one has the annealed variables which reach equilibrium on experimental timescales (e.g., spins), and the quenched variables that can usually be considered frozen from observational purposes (e.g., exchange interactions) [1, 2], whereas in biology one has the ecological variables (e.g., species abundances) and the evolutionary variables (e.g., characteristics of the species) [3]. The analogy is made stronger by noting that the features that distinguish a species from the others also determine the strengths (and signs as well) of the interspecies interactions.

Most population dynamics as well as spin-glass models have focused on the characterization of the properties of the fast variables only, although at least in the biology context it is obvious that the main drive for changing a species should come from the outcome of the competition in the ecological domain. A more suitable framework would allow the slow

variables to vary so as to reach equilibrium together with the fast variables, while keeping the two timescales apart. (In the annealed approximation of statistical physics, both spins and interactions are viewed as fast variables evolving on the same timescale.) A mathematical framework to treat this intermediate situation—termed as partial annealing—based on the standard statistical mechanics tools was put forward independently by Coolen *et al* [4, 5] and Dotsenko *et al* [6]. Those contributions unveiled a new physical interpretation for the number of replicas n: it is proportional to the ratio $\tilde{\beta}/\beta$ between the inverse temperatures characterizing the Boltzmann distributions of the slow and fast variables.

In this paper, we use the partial annealing framework to study the effect of the slow relaxation of the interspecies interactions on the equilibrium properties of a well-known ecosystem model—the random replicator model [7]. Following the population dynamics tradition, this model and its variants have been extensively studied within the equilibrium statistical mechanics framework in the case of the quenched interactions [8–11]. In the partial annealing approach, the quenched limit is recovered by setting $\tilde{\beta} = 0$ and hence $n = 0$ [4–6]. Since the random replicator model is defined for the deterministic regime $\beta \to \infty$ only, in this contribution we focus on the limit $n \sim \beta^{-1} \to 0$ such that the product $n\beta$ is finite and proportional to $\tilde{\beta}$.

We find that the slow change of the interspecies interactions, which is primarily driven by the strength of the correlations between species, may alter radically the equilibrium properties of the ecosystem as compared with the static, quenched case. This happens in the case where alliances of pairs of abundant species are favoured by the coupled dynamics of the interspecies interactions and species abundances, leading to the onset of a discontinuous transition between a regime of high species diversity and a regime of zero diversity. In addition, we find that the replica-symmetric approach fails dramatically to describe the situation where the intensity of the competition increases as a species becomes more abundant, which corresponds to negative values of the replica number. In this case, species alliances cannot be formed, then resulting in richer ecosystems.

2. Random replicator model

The abundance of individuals of species $i = 1, \ldots, N$ in the ecosystem is described by the real-valued quantity $x_i \in [0, \infty)$ and the form the encounter between the ith and jth species affects the growth of species i is given by the interspecies interaction strength J_{ij}. In the ecological timescale, the interactions are held fixed and the species concentrations change following the replicator equation [12, 13]

$$\frac{\mathrm{d}x_i}{\mathrm{d}t} = x_i(\mathcal{F}_i - \phi), \tag{1}$$

where $\mathcal{F}_i = -\sum_j J_{ij}x_j$ can be identified with the fitness of species i and ϕ is a Lagrange multiplier that enforces the constraint

$$\sum_{i=1}^{N} x_i = N \tag{2}$$

for all t. Species j will tend to decrease the abundance of species i if $J_{ij} > 0$, whereas it will promote the growth of species i if $J_{ij} < 0$.

In the case of *symmetric* interactions $J_{ij} = J_{ji}$, the asymptotic regime of equation (1) can be fully described by examining the maxima of a fitness functional $\mathcal{F}$ or, equivalently, the minima of the Hamiltonian $\mathcal{H}$ defined by [7]

$$\mathcal{F}(\{J_{ij}\}, \{x_i\}) = -\mathcal{H}(\{J_{ij}\}, \{x_i\}) = -\frac{1}{2}\sum_{i,j} J_{ij}x_i x_j \tag{3}$$

and so it can be shown that the only stationary states are fixed points (see, e.g., [13]). In this case, the Lagrange multiplier in equation (1) is the mean fitness of the ecosystem, i.e., $\phi = \frac{1}{N}\sum_i x_i\mathcal{F}_i$. Because of this symmetry assumption, we can sort out the pairs of species into two categories: competing species for which $J_{ij} > 0$ and cooperating species for which $J_{ij} < 0$.

Assuming that the symmetric interspecies interactions are statistically independent random variables, we can easily obtain the equilibrium properties of the ecosystem model within the statistical mechanics approach [7]. The basic idea is to introduce the partition function

$$Z(\{J_{ij}\}) = \int_0^\infty \prod_i \mathrm{d}x_i \delta\left(N - \sum_i x_i\right) \exp[-\beta\mathcal{H}(\{J_{ij}\}, \{x_i\})] \tag{4}$$

and then focus on the zero-temperature limit $\beta = 1/T \to \infty$ to ensure that only the states that minimize $\mathcal{H}$ will contribute to Z.

3. Partial annealing formalism

As pointed out before, the ecosystem model described by equations (1)–(3), termed the random replicator model, has been extensively studied in the case the interspecies interactions are quenched (fixed) variables. Here, we study analytically a more realistic situation in which the interactions J_{ij} evolve on a much slower timescale, the evolutionary timescale, than the characteristic timescale associated with the change of the species concentrations x_i, the ecological timescale. Following Coolen *et al* [4], we assume that the species concentrations are effectively in equilibrium on the timescale of the interactions dynamics. This equilibrium is characterized by the Boltzmann distribution

$$\mathcal{P}(\{J_{ij}\}, \{x_i\}) = \frac{1}{Z}\delta\left(N - \sum_i x_i\right) \exp[-\beta\mathcal{H}(\{J_{ij}\}, \{x_i\})] \tag{5}$$

with Z given by equation (4).

The partial annealing approach is based on the assumption that the interspecies interactions J_{ij} evolve according to the equation

$$\tau\frac{\mathrm{d}}{\mathrm{d}t}J_{ij} = \frac{\epsilon}{N}\langle x_i x_j\rangle_J - \mu J_{ij} + \frac{1}{\sqrt{N}}\eta_{ij}(t), \qquad i < j, \tag{6}$$

where $\epsilon = \pm 1$ and the notation $\langle\cdots\rangle_J$ stands for the thermal average taken with the distribution (5). Here, η_{ij} is a Gaussian noise of zero mean and covariance

$$\overline{\eta_{ij}(t)\eta_{kl}(t')} = 2\tau\tilde{\beta}^{-1}\delta_{(i,j),(kl)}\delta(t - t') \tag{7}$$

which introduces the characteristic inverse temperature of the interaction system, $\tilde{\beta}$. In the first term on the right-hand side of equation (6), the choice $\epsilon = -1$ corresponds to a Hebbian-like reinforcement process [14]: the larger the correlation $\langle x_i x_j\rangle_J$ between the species i and j, the more negative the J_{ij} becomes, promoting thus the mutual growth of both species. The case $\epsilon = +1$ is more interesting since it corresponds to a situation where competition prevails—any

two abundant species will become fiercer competitors and so try to deplete the concentration of each other. Finally, the term $-\mu J_{ij}$ in equation (6) prevents the unbounded growth of the magnitudes of the interactions and the quantity τ ensures that this equation is dimensionally homogeneous.

The coupling between the species concentrations and the interspecies interactions is due solely to the term $\langle x_i x_j \rangle_J \geqslant 0$ which can be eliminated from equation (6) using the identity

$$\langle x_i x_j \rangle_J = -\frac{1}{\beta} \frac{\partial}{\partial J_{ij}} \ln Z(\{J_{ij}\}) \tag{8}$$

so that the coupling dynamics can be written in the form of a Langevin equation,

$$N\tau \frac{\mathrm{d}}{\mathrm{d}t} J_{ij} = -\frac{\partial}{\partial J_{ij}} \tilde{\mathcal{H}}(\{J_{ij}\}) + \sqrt{N}\eta_{ij}, \qquad i < j, \tag{9}$$

where we have defined the effective Hamiltonian

$$\tilde{\mathcal{H}}(\{J_{ij}\}) = \frac{\epsilon}{\beta} \ln Z(\{J_{ij}\}) + \frac{N\mu}{2} \sum_{k<l} J_{kl}^2. \tag{10}$$

Hence, the equilibrium distribution of the interaction system is also a Boltzmann distribution, $\tilde{\mathcal{P}}(\{J_{ij}\}) = \exp[-\tilde{\beta}\tilde{\mathcal{H}}(\{J_{ij}\})]/\tilde{Z}$, where

$$\tilde{Z} = \int_{-\infty}^{\infty} \prod_{i<j} \mathrm{d}J_{ij} \exp[-\tilde{\beta}\tilde{\mathcal{H}}(\{J_{ij}\})]. \tag{11}$$

The delicacy of the partial annealing formulation can be appreciated when equation (10) is inserted into the above expression for the partition function of the interaction system, yielding

$$\begin{aligned} \tilde{Z} &= \int_{-\infty}^{\infty} \prod_{i<j} \mathrm{d}J_{ij} [Z(\{J_{ij}\})]^n \exp\left(-\frac{1}{2}\tilde{\beta} N\mu \sum_{i<j} J_{ij}^2\right) \\ &= \left(\frac{2\pi}{\tilde{\beta} N\mu}\right)^{N(N-1)/4} \langle [Z(\{J_{ij}\})]^n \rangle, \end{aligned} \tag{12}$$

where $n = -\epsilon\tilde{\beta}/\beta$ and the notation $\langle \cdots \rangle$ stands for the average over the random independent Gaussian variables J_{ij} of zero mean and variance $1/\tilde{\beta} N\mu$. Aside from a trivial additive factor of the order of $N^2 \ln N$, which gives the dominant contribution to the global free energy $\tilde{F}$ defined by

$$-\tilde{\beta}\tilde{F} = \ln \tilde{Z}, \tag{13}$$

the evaluation of the terms of order N in the free energy can easily be carried out by resorting to the very same tricks used in the case of quenched disorder [1, 2]. In that case, however, n has no apparent physical meaning—it is an auxiliary parameter that appears in the identity $\langle \ln y \rangle = \lim_{n\to 0} \frac{1}{n} \ln \langle y^n \rangle$.

To obtain the standard results of the quenched limit for the Gaussian-distributed interactions [7], it is not enough to set $\tilde{\beta} = 0$, thus implying that the interactions dynamics, equation (6), is governed by the noise term η_{ij}. The reason is that the variance of the interactions distribution depends on $\tilde{\beta}$ (see equation (12)) and so it would vanish in the required limit. The partial annealing formulation of Dotsenko *et al* [6] circumvents this difficulty by setting $\mu = 1/\tilde{\beta}$. In this paper, we follow this prescription so that the dependence of $\tilde{Z}$ on $\tilde{\beta}$ occurs through n only. Since the relevant limit for the replicator dynamics is $\beta \to \infty$, n must tend to 0 such that the product $\beta n = -\epsilon\tilde{\beta}$ is finite. To facilitate the presentation of the results, we introduce an effective inverse temperature $\beta' = -\epsilon\tilde{\beta}$ which can take on positive as well as negative values.

Finally, to prevent the unbounded growth of any single species—a possibility in the limit $N \to \infty$—we introduce a quadratic damping term that accounts for the self-limitation in the growth of each species. This is achieved by setting $J_{ii} = u > 0$ for all i. Henceforth, u will be referred to as the intraspecies competition parameter.

4. Replica approach

The trick to carry out the average over the interactions in equation (12) is to evaluate $[Z(\{J_{ij}\})]^n$ for *integer* n first, then calculate the integrals over J_{ij} explicitly and finally make the naive analytical continuation to the real negative or positive n (see [15] for the justification of this procedure). The evaluation of the terms of order N in equation (13) is standard by now, so we present the final result only,

$$-\tilde{\beta}\tilde{F}/N = \sum_a Q_a(\beta^2\hat{Q}_a + \beta^2 Q_a/4 - \beta u/2) - \beta^2 \sum_{a<b} q_{ab}(\hat{q}_{ab} - q_{ab}/2) + \beta \sum_a \hat{R}_a + \ln G(\hat{R}_a, \hat{Q}_a, \hat{q}_{ab}), \tag{14}$$

where

$$G = \int_0^\infty \prod_a \mathrm{d}x_a \exp\left[-\beta \sum_a \hat{R}_a x_a - \beta^2 \sum_a \hat{Q}_a x_a^2 + \beta^2 \sum_{a<b} \hat{q}_{ab} x_a x_b\right]. \tag{15}$$

At this stage, the replica indices a and b run from the integers 1 to n, and the saddle-point parameters Q_a, $\hat{Q}_a$, q_{ab}, $\hat{q}_{ab}$ and $\hat{R}_a$ are chosen so as to minimize the total free energy $\tilde{F}$. The relevant physical order parameters are

$$q_{ab} = \frac{1}{N}\sum_i \langle \langle x_{ia} x_{ib} \rangle_T \rangle, \qquad a < b \tag{16}$$

and

$$Q_a = \frac{1}{N}\sum_i \langle \langle x_{ia}^2 \rangle_T \rangle, \tag{17}$$

which measure the overlap between a pair of stationary states labelled by the replica indices a and b, and the overlap between the stationary state labelled by a with itself, respectively. Here, $\langle \cdots \rangle_T$ stands for a thermal average taken with the Boltzmann distribution $\tilde{\mathcal{P}}(\{J_{ij}\})$. The other parameters, $\hat{R}_a$, $\hat{Q}_a$ and $\hat{q}_{ab}$, enter the calculation as Lagrange multipliers. To proceed further and carry out the analytical continuation to real n, we must make some simplifying assumption about the structure of the saddle-point parameters.

4.1. Replica-symmetric solution

The simplest conjecture is that the saddle-point parameters are symmetric under permutations of the replica indices, i.e., $q_{ab} = q, \hat{q}_{ab} = \hat{q}, Q_a = Q, \hat{Q}_a = \hat{Q}$ and $\hat{R}_a = \hat{R}$. This prescription allows the explicit evaluation of the integrals in equation (15) resulting in the following replica-symmetric free energy density, $\tilde{f} = \tilde{F}/N$,

$$-\tilde{\beta}\tilde{f}/n = Q(\beta^2\hat{Q} + \beta^2 Q/4 - \beta u/2) - \frac{1}{2}(n-1)\beta^2 q(\hat{q} - q/2) + \beta\hat{R} - \frac{1}{2}\ln(\hat{Q} + \hat{q}/2) + \frac{1}{n}\ln \int_{-\infty}^{\infty} Dz \left[\exp\left(\Xi_z^2\right)\mathrm{erfc}\left(\Xi_z\right)\right]^n, \tag{18}$$

where

$$\Xi_z = \frac{\hat{R} - \hat{q}^{1/2} z}{2(\hat{Q} + \hat{q}/2)^{1/2}}, \tag{19}$$

$$Dz = \frac{dz}{(2\pi)^{1/2}} \exp(-z^2/2), \tag{20}$$

and we have neglected trivial additive terms. Note that at this stage n can be considered a real variable. The saddle-point parameters q, Q, $\hat{R}$, $\hat{q}$, $\hat{Q}$ are obtained by solving the five coupled nonlinear equations that result from extremizing the free energy with respect to each of them. Since our aim is to single out the states that maximize the fitness functional (3) for a fixed set of interactions, we must consider the zero-temperature limit $\beta \to \infty$ of the saddle-point equations taking care to take the dependence of n on β, $n = -\epsilon\tilde{\beta}/\beta = \beta'/\beta$, into account. The limit is taken such that $\lim_{\beta\to\infty} 2\beta(\hat{Q} + \hat{q}/2) = u - v$, where $v = \lim_{\beta\to\infty} \beta(Q - q)$ is finite. As a result, $\Xi_z \propto \beta^{1/2} \to \pm\infty$, so the complementary error function can be replaced by its asymptotic form. After some algebra, we can reduce the set of saddle-point equations to the following three coupled equations:

$$(u - v) = Q^{1/2} \frac{\phi_1}{\int_{-\infty}^{\Delta} Dz + \phi_0}, \tag{21}$$

$$(u - v)^2 = \frac{\phi_2}{\int_{-\infty}^{\Delta} Dz + \phi_0}, \tag{22}$$

$$\Delta = Q^{1/2}(2v - u + \beta' Q), \tag{23}$$

where

$$\phi_m = \int_{\Delta}^{\infty} Dz \exp\left[\frac{\alpha}{2}(z - \Delta)^2\right](z - \Delta)^m, \tag{24}$$

with $\alpha = \beta' Q/(u - v)$. These saddle-point equations must be solved for the physical parameters Q and v, as well as for the auxiliary parameter $\Delta = \hat{R}/\hat{q}^{1/2}$. In the replica-symmetric framework, definitions (16) and (17) become

$$q = \frac{1}{N} \sum_i \langle \langle x_i \rangle_T^2 \rangle, \tag{25}$$

$$Q = \frac{1}{N} \sum_i \langle \langle x_i^2 \rangle_T \rangle, \tag{26}$$

where the thermal average is now calculated using the replica-symmetry prescription. Hence, $v \propto Q - q > 0$ can be interpreted as a susceptibility that measures the fluctuations around the average species concentration, whereas Q is proportional to the probability that two randomly selected individuals belong to the same species, a measure known as Simpson index in the ecology literature [16]. Henceforth, we will refer to Q as the Simpson index, though, strictly, the correct definition of that index is Q/N. Clearly, Q gives an indication of the distribution of species in the ecosystem: large Q means that a few species dominate the ecosystem whereas Q close to 1 means that most of the N species are present in the ecosystem in approximately equal concentrations. It is interesting to note that the Simpson index is related to the Rényi entropy [17]

$$\mathcal{S}_\gamma = \frac{1}{1 - \gamma} \ln \left[\sum_i^N (x_i/N)^\gamma \right] \tag{27}$$

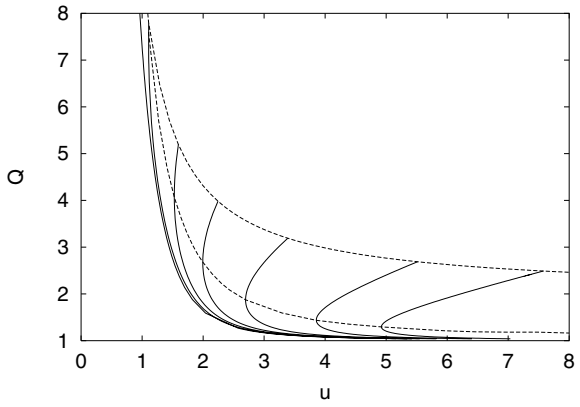

Figure 1. Simpson index Q as a function of the intraspecies competition parameter u for (solid curves from left to right) $\beta' = 0, 0.1, 0.25, 0.5, 1, 2$ and 3. The upper dashed curve corresponds to the condition $\alpha = 1$. The lower dashed curve marks the values of u beyond which the saddle-point equations have two solutions. The large Q solution (upper branch) is unstable to fluctuations within the replica-symmetric space.

for $\gamma = 2$. We recall that the Rényi entropy reduces to the Shannon entropy in the limit $\gamma \to 1$.

The free energy in this limit becomes

$$-\epsilon \tilde{f} = Q\left(u - \frac{3}{2}v + \frac{\beta'}{4}Q\right) + \frac{1}{\beta'}\ln\left(\int_{-\infty}^{\Delta} Dz + \phi_0\right). \tag{28}$$

The results for the quenched case can be easily recovered by setting $\beta' = 0$ (and hence $\alpha = 0$) in the saddle-point equations, equations (21)–(23), and in the free energy, equation (28).

4.2. Stability of the replica-symmetric solution

In using the replica-symmetry prescription to evaluate the saddle-point parameters, it is important to check that the solution is in fact locally stable. An instability of the replica-symmetric solution is determined by a sign change in (at least) one of the eigenvalues of the matrix of quadratic fluctuations around the replica-symmetric solution. Following the standard stability analysis [18], we find that the stability against perturbations that break the replica symmetry is given by the de Almeida–Thouless condition

$$\frac{1}{(u-v)^2}\frac{\phi_0}{\int_{-\infty}^{\Delta} Dz + \phi_0} < 1. \tag{29}$$

4.3. Analysis of the results

The set of saddle-point equations can be easily solved numerically by changing the status of the variables u and Δ so that the latter is viewed as a known, given parameter and the former as an unknown. Varying Δ from $-\infty$ to ∞ allows us to sweep the entire range of physical values of u. In what follows, we will focus on the dependence of the Simpson index Q on β' and u.

The results for $\beta' > 0$ are summarized in figure 1. Since ϕ_m diverges for $\alpha > 1$, the saddle-point equations become invalid in this regime and so the extreme of the free energy is

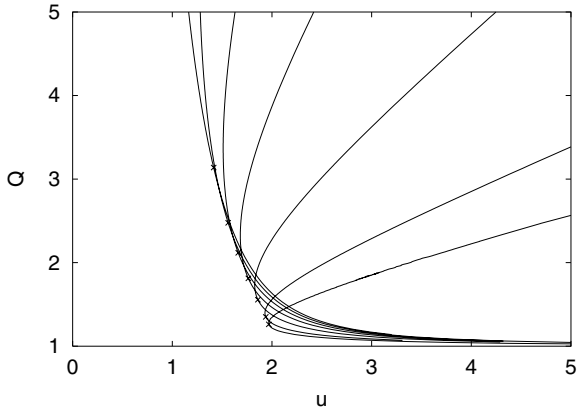

Figure 2. Simpson index Q as a function of the intraspecies competition parameter u for (solid curves from left to right) $\beta' = 0, -0.1, -0.25, -0.5, -1, -2$ and -3. The symbols $\times$ indicate the instability of the replica-symmetric solution.

obtained for $Q \to \infty$. For $\alpha = 1$, the saddle-point equations have a finite solution, represented by the upper dashed curve in figure 1. Because of this divergence, the saddle-point equations can have zero, one or two solutions for fixed u. Actually, only the lower branch solution (small Q) is stable against fluctuations within the replica-symmetric space, so the transition from finite Q to $Q \to \infty$ takes place at the lowest value of u for which the saddle-point equations have solution. This corresponds to the lower dashed curve in figure 1. For $\beta' < 0.1$ these two curves coincide. In addition, we find that condition (29) is always satisfied by the replica-symmetric solutions (upper and lower branches), so these solutions are stable against fluctuations that take them outside the replica-symmetric space. This is in agreement with the findings for the spherical spin-glass model, for which the replica-symmetric solution was proved to be stable for positive n [19].

In figure 2 we sum up the results for $\beta' < 0$. Since $\alpha \leqslant 0$, there is no risk of divergence in the evaluation of ϕ_m and so the saddle-point equations have either zero or two solutions for fixed u. In this case, however, the upper branch solution is always unstable to fluctuations that break the replica symmetry, as indicated in the figure. In particular, we find that the instability sets in at $u = \sqrt{2}$ for $\beta' = 0$ and at $u = 2$ for $\beta' \to -\infty$. The results are qualitatively similar to those for $\beta' > 0$ as in both cases there is no solution to the saddle-point equations (thus implying $Q \to \infty$) for small u. This is in stark contrast with the quenched case for which Q diverges at $u = 0$ only. The phase diagram depicted in figure 3 summarizes the main results. Note that for $\beta' < 0$ the lower branch solution (small Q solution) becomes unstable before the onset of the discontinuous transition to a regime characterized by $Q \to \infty$. We will argue in section 8, however, that for $\beta' < 0$ this transition is an artefact of the replica-symmetric solution: the correct solution should correspond to a finite Q value which is upper-bounded by the quenched solution. Finally, we note that for $\beta' = 0$ the saddle-point equations have a single solution in the entire range of u.

5. Distribution of the species abundances

The measure of the relative abundance of each species is a classic form to investigate the structure of the ecosystem. For instance, studies based on samples of insects [20] and plants

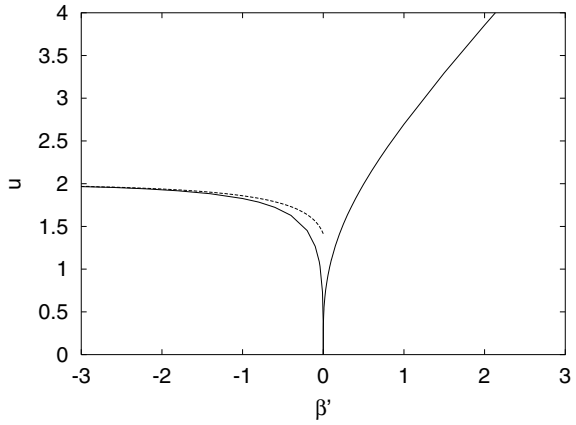

Figure 3. Phase diagram in the plane (β', u). The dashed curve for $\beta' \leqslant 0$ is the de Almeida–Thouless line—the replica-symmetric (RS) solution is stable above this line. The solid curves signal the limit of the existence of a solution with the finite saddle-point parameters. The RS solution is stable for $\beta' > 0$.

[21] led to the conclusion that their abundances are distributed geometrically, i.e., most species are relatively rare, whereas a few species are fairly common. In general, however, the log-normal distribution, that describes the situation in which the most numerous category contained species of intermediate abundance, seems more adequate to fit survey data, especially in thoroughly censused communities [22].

To calculate the cumulative distribution that the concentration of a given species takes on a value smaller than x, denoted by $C(x)$, we must assume first that all species concentrations are identically distributed, so we can add an extensive term $h\sum_i \Theta(x - x_i)$ to the Hamiltonian (3). The desired cumulative distribution can be obtained by taking the derivative of the resulting free energy with respect to h and then setting $h = 0$. The final result is

$$C(x) = 1 - \frac{\int_{\Delta + x(u-v)/Q^{1/2}}^{\infty} Dz \exp\left[\frac{\alpha}{2}(z-\Delta)^2\right]}{\int_{-\infty}^{\Delta} Dz + \phi_0}, \tag{30}$$

from where we can obtain the fraction of surviving species in the ecosystem at equilibrium, i.e., the diversity $d = 1 - C(0)$,

$$d = \frac{\phi_0}{\int_{-\infty}^{\Delta} Dz + \phi_0}. \tag{31}$$

Note that $C(0) > 0$ implies that the probability density that the abundance of a certain species is x exhibits a delta peak at $x = 0$, i.e., $P(x) = \delta(x)C(0) + \mathrm{d}C(x)/\mathrm{d}x$.

In figure 4, we present the dependence of the diversity on the control parameters of the model. Of course, all threshold and instability phenomena that affect the Simpson index Q influence the diversity d as well, as illustrated in the figure. In particular, $d = 0$ in the regime where the extremum of the free energy is obtained for $Q \to \infty$. As expected, the large values of the intraspecies competition parameter lead to a maximum of the diversity. A typical distribution of abundances of the surviving species is presented in figure 5, from where we can see that the species of intermediate abundance are the most numerous, in agreement with the field observations [22]. In addition, low abundance species are favoured in the case of $\beta' > 0$

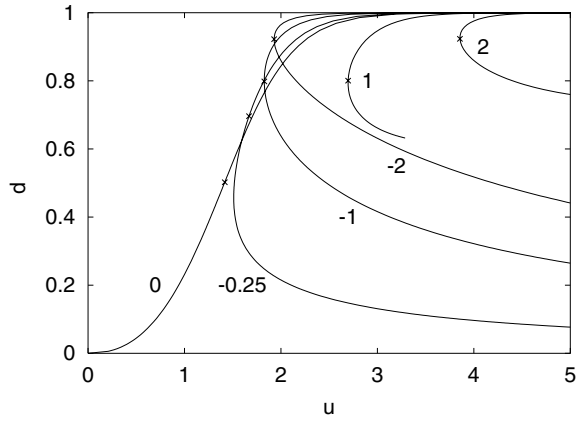

Figure 4. Fraction of surviving species in the ecosystem for the values of β' indicated in the figure. The symbol $\times$ signals the limit of validity of the solutions.

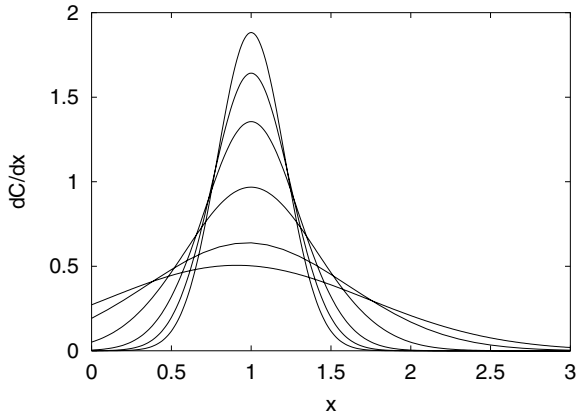

Figure 5. Finite part of the distribution of abundance for $u = 3$ (top to bottom at $x = 1$), $\beta' = -6, -4, -2, 0, 1$ and 1.2.

and strongly penalized for $\beta' < 0$. We leave the appraisal of the consequences of these results to section 8.

6. Distribution of the interspecies interactions

Since the interactions J_{ij} are dynamic variables, it would be desirable to characterize their equilibrium statistical properties as well. The integration over the interactions already in the first stage of the calculation of the free energy precludes the manifestation of the saddle-point parameters that could inform us about the organization of the space of interactions at equilibrium. In this section, we focus on the first moments of the probability distribution of a single interaction coupling, say J_{kl}. This distribution is defined by integrating the Boltzmann distribution, $\tilde{\mathcal{P}}(\{J_{ij}\})$, over all J_{ij} except J_{kl}. Of course, since the species are equivalent, all couplings are identically distributed and so we can consider the quantities

$M_m = \frac{1}{N}\left\langle \sum_{i<j} J_{ij}^m \right\rangle$ with $m = 1, 2, \ldots$ instead, which are much easier to calculate. For example, we can easily derive from equation (6) that $M_1 = -\beta'(1 - Q/N)/2$. In addition, taking the derivative of $\ln \tilde{Z}$ with respect to μ (see equation (12)) and setting $\mu = 1/\tilde{\beta}$ yields $M_2 = \frac{1}{2} + \frac{1}{2N}[\beta'(2vQ + \beta' Q^2) - 1]$. These results imply that $\langle J_{kl} \rangle \approx -\beta'/N$ and $\left\langle J_{kl}^2 \right\rangle \approx 1/N$ for large N.

Aside from the calculation of M_1, equation (6) does not yield to an analytical approach because $\langle x_i x_j \rangle_J$ depends on the entire set of couplings $\{J_{ij}\}$. Estimate of M_3 using simulations (see the next section) yields $\left\langle J_{kl}^3 \right\rangle \approx -3\beta'/N^2$ indicating thus that the third cumulant will vanish as $1/N^3$ in the thermodynamic limit. This finding prompts the conjecture that J_{kl} follows a Gaussian distribution for large N. (We recall that for $\beta' = 0$ the distribution of J_{kl} is a Gaussian of zero mean and variance $1/N$.) Of course, what really matters to the equilibrium properties of the ecosystem for $\beta' \neq 0$ are the nontrivial correlations between different interactions produced by the deterministic term $\langle x_i x_j \rangle_J$ in equation (6). This is the reason that the properties of the ecosystem for $\beta' \neq 0$ differ so markedly from those of the quenched case.

7. Simulations

Ecosystem models are usually defined by the equations that govern the dynamics of their constituent species, so it is important to confirm that the equilibrium analysis carried out in the previous sections yields in fact the stationary states of the rather complex coupled dynamics of interactions and species abundances. A purely dynamic approach, that conforms with our work assumption that the concentrations of the species $\{x_i\}$ evolve much faster than the interspecies interactions $\{J_{ij}\}$, consists in solving the replicator dynamics (1) for fixed interactions, calculating the products $x_i x_j$ for all pairs $i < j$, and then updating the interactions according to equation (6).

As the focus of this paper is on the limit $\beta \to \infty$, we find it more efficient to search for the minima of $\mathcal{H}$ in equation (3) directly, instead of solving the differential equations (1). This search is performed as follows. Starting from the uniform situation $x_i = 1 \forall i$, we pick a pair of species at random, say i and k, and set $x_i' = x_i + \zeta$ and $x_k' = x_k - \zeta$ with $\zeta = 0.01$. If this change results in the decrease of $\mathcal{H}$ then the modification becomes effective (i.e., x_i' and x_k' replace x_i and x_k), otherwise it is discarded and a new pair of species is chosen. In the case that $x_k' < 0$, we reset $x_k' = 0$ and $x_i' = x_i + x_k$. In addition, if any of the species concentrations, x_i or x_k, happen to be zero we pick out another pair, thus guaranteeing that there is no recovery from extinction. This procedure is repeated until no further decrease of $\mathcal{H}$ is possible. For this minimum energy configuration, the products $x_i x_j, \forall i < j$, are computed and then used to evolve the interspecies interactions with the Euler method with time step $\Delta t = \tau\delta$. The initial condition for the interactions is $J_{ij} = 0, \forall i < j$. We can set $\tau = 1$ without loss of generality but the value of δ (here we set $\delta = 0.01$) influences the Gaussian noise term in (6), such that $\mathrm{var}(\eta) \sim \delta^{-1}$ [5]. The entire process (minimization of $\mathcal{H}$ and a single time update in $J_{ij} \forall i < j$) is repeated 10^4 times to allow for thermal equilibration of the interactions. After this initial transient period, we follow the system evolution for about 10^4 additional iterations and record the quantities of interest—the Simpson index and the moments of the distribution of J_{ij}.

In figure 6, we show that even for small system sizes ($N = 80$) the agreement between the analytical predictions for the Simpson index and the simulation results is excellent in the parameter region where the replica-symmetric saddle point is stable, which comprehends the entire range of u for $\beta' > 0$. The numerical estimate of the moments of the distribution of the interactions is somewhat more delicate because in the expression for the rescaled

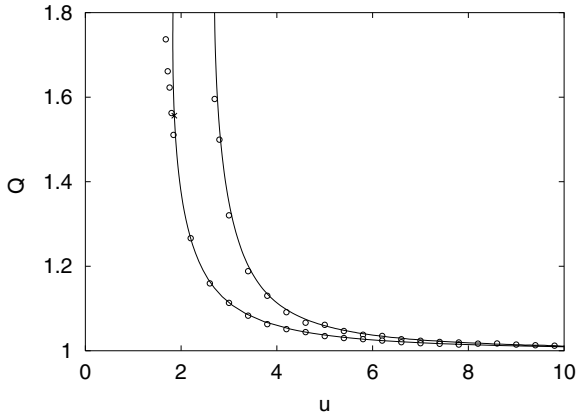

Figure 6. Comparison between the replica-symmetric estimate for the Simpson index Q (solid curves) and the simulations of an ecosystem with $N = 80$ species (○) for $\beta' = -1$ (left curve) and $\beta' = 1$ (right curve). The error bars are smaller than the symbol sizes. The symbol × indicates the location of de Almeida–Thouless instability point for $\beta' = -1$.

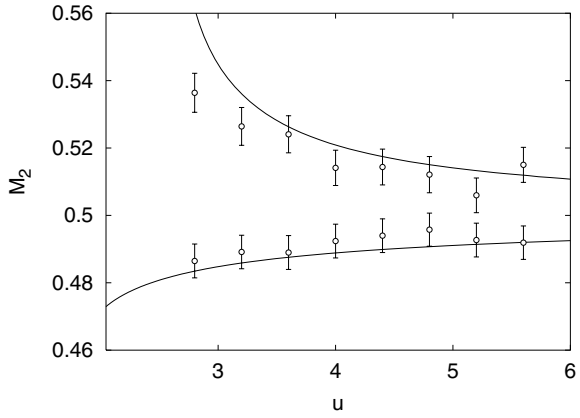

Figure 7. Comparison between the rescaled second moment of J_{ij} as predicted by the replica-symmetric calculation (solid curves) and the simulations with $N = 20$ species (○) for $\beta' = -1$ (lower curve) and $\beta' = 1$ (upper curve). For $N \to \infty$, $M_2 \to 1/2$ regardless of the values of u and β'.

moments M_m (see section 6) only the terms on the order of $1/N$ exhibit a nontrivial dependence on the control parameters of the model. To enhance the finite N effects, in figure 7 we present the results for an ecosystem comprising $N = 20$ species only. The agreement between theory and simulations is reassuring in the sense it shows that the statistical mechanics analysis can provide valuable insights into the statistical properties of small systems as well.

As mentioned before, to obtain the dependence of M_3 on the control parameters β' and u, as well as on the system size N, we have to recourse to simulations. Fortunately, to the leading order in N the simulation results summarized in figure 8 are uncontroversial. In contrast to M_1 and M_2 which tend to nonzero asymptotic values in the thermodynamic limit, M_3 decreases as $1/N$ keeping the product $NM_3 = -3\beta'/2$ independent of u.

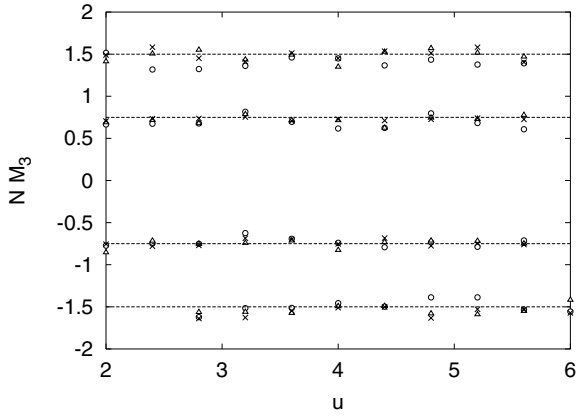

Figure 8. Simulation results of the rescaled third moment of J_{ij} for different ecosystem sizes, $N = 20$ ($\circ$), $N = 40$ ($\triangle$), $N = 80$($\times$) and (top to bottom) $\beta' = -1, -0.5, 0.5$ and 1. The error bars are smaller than the symbol sizes. The horizontal dashed lines are the fittings $NM_3 = -3\beta'/2$.

8. Discussion

The most noticeable result of the previous analysis is the harmful effect of $\beta' > 0$ (or $\epsilon = -1$) on the diversity of the ecosystem (see figures 1 and 4). A finite value of the Simpson index Q is obtained only for relatively large values of the intraspecies competition parameter u, which prevents the unlimited growth of the species. The reason for that can be apprehended by inspection of equation (6): a pair of species, say i and j, of high abundances (i.e., $\langle x_i x_j \rangle_J \gg 1$) induces negative interaction strengths J_{ij} between them, which in turn promotes further growth of their abundances. This is a positive feedback loop which results in the explosive growth of species i and j and, consequently, in the extinction of the other species due to constraint (2). In fact, we find in the simulations that $Q \approx N/2$ for small u indicating the presence of a single pair of species in the ecosystem. In addition, figure 5 corroborates this scenario by showing that there is a significant increase in the probability of finding low and high abundance species in the ecosystem, as compared with the case $\beta' \leqslant 0$.

The interpretation of the results for $\beta' < 0$ (or $\epsilon = 1$) is more delicate because the replica-symmetric solution is unreliable in the range of u where the stability condition (29) is violated. In this case, there is a mechanism of negative feedback that should restrain the species abundances from uncontrolled growth. In fact, this mechanism is effective in the region where the replica-symmetric solution is stable, as reflected by the high values of the diversity measure and the low values of the Simpson index as compared with those for the quenched case (see figures 2 and 4). The distribution of species abundances shown in figure 5 confirms this restrictive effect as both high and low abundance species are very unlikely to be found in the ecosystem. Hence, in contrast with the case $\beta' > 0$, there is no apparent physical mechanism to explain a sudden reduction of the diversity as predicted by the replica-symmetric solution. In contrast, the above reasoning indicates that the ecosystem diversity should be higher than the diversity in the quenched case. To clarify this issue, in figure 9 we present a comparison between the simulation estimates of the Simpson index for $\beta' = 0$ and $\beta' = -1$. As expected, for fixed N and u the results for $\beta' = 0$ are upper bounds to those for $\beta' = -1$.

The spectacular failure of the replica-symmetric approach to predict the equilibrium properties of the ecosystem for small u in the case $\beta' < 0$ may be explained by a discontinuous

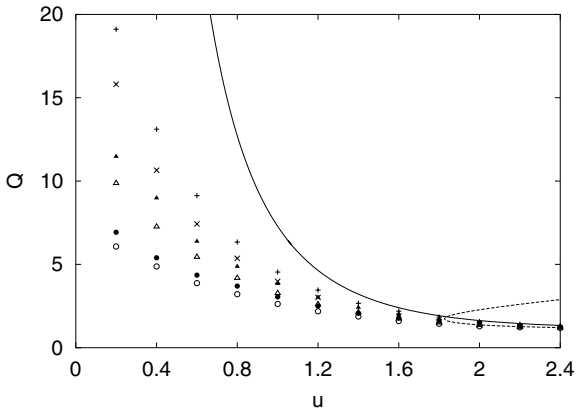

Figure 9. Effect of the finite ecosystem size on the Simpson index for $\beta' = -1$ ($N = 20$ (○), $N = 40$ (△), $N = 80$(×)) and $\beta' = 0$ ($N = 20$ (●), $N = 40$ (▲), $N = 80$ (+)). The error bars are smaller than the symbol sizes. The solid and dashed curves are the replica-symmetric predictions for $\beta' = 0$ and $\beta' = -1$, respectively.

phase transition between the replica symmetry and replica-symmetry broken regimes. This interesting possibility will be investigated in a future contribution.

9. Conclusion

Unlike most population dynamics models in which the interspecies interactions are fixed *a priori*, the ecosystem model studied in this contribution addresses a more general situation in which both species concentrations x_i and interactions J_{ij} change with time, albeit in widely separated timescales. The equilibrium of the coupled dynamics of concentrations and interactions can be described by the partial annealing formalism of the statistical physics of disordered systems [4–6], provided two conditions are satisfied. First, the interactions must be symmetric $J_{ij} = J_{ji}$ so that for fixed interactions the equilibrium of the species concentrations is described by the Boltzmann distribution (5). This allows the classification of pairs of species in cooperative ($J_{ij} < 0$) and competitive ($J_{ij} > 0$) pairs. Second, the species concentrations at equilibrium must affect the interactions rate $\mathrm{d}J_{ij}/\mathrm{d}t$ only through their pairwise correlations $\epsilon\langle x_i x_j\rangle_J$ (see equation (6)), so that one can define an effective Hamiltonian for the interactions.

The equilibrium properties of the ecosystem depend mainly on the sign of ϵ. On the one hand, the choice $\epsilon = -1$ favours the appearance of alliances between pairs of highly abundant species: unless the intraspecies competition is sufficiently high, the positive reinforcement mechanism will eventually lead to the complete dominance of a single pair of species. This is reflected by the appearance of a discontinuous transition between a regime characterized by a finite value of the Simpson index Q and a regime where $Q \to \infty$ with the consequent vanishing of the ecosystem diversity. The spontaneous formation of defensive alliances between subgroups of species has also been reported in more realistic ecological models in which the interspecies interactions are determined by cyclic food webs (see, e.g., [23, 24]).

The choice $\epsilon = +1$, on the other hand, models the case where the strength of the competition that a species experiences from all other species in the ecosystem is proportional to its abundance, so it pays to keep a low profile. For low levels of the intraspecies competition, the replica-symmetric approach fails to describe the equilibrium for $\epsilon = 1$, which corresponds

to the negative replica numbers, and so our conclusions are based on extensive simulations of the coupled dynamics.

Since $\langle J_{ij} \rangle \approx \beta'/N = \epsilon\tilde{\beta}/N$, ultimately it is the sign of ϵ that determines whether any two species will cooperate or compete with each other. Hence, by fixing ϵ (or β') we are left with an ecosystem model where the interspecies interactions are predominantly competitive ($\beta' < 0$) or cooperative ($\beta' > 0$), whereas a more realistic situation would be characterized by a balance between these two types of interactions. Such a situation could be studied by considering ϵ as a random variable, which amounts to considering the replica number n as a quenched random variable as well.

As in the context of attractor neural networks (see, e.g., [14]), the assumption that the interspecies couplings (or synaptic weights in that context) J_{ij} are symmetric is utterly unrealistic from the biological viewpoint but, on the other hand, it allows a full equilibrium statistical mechanics analysis of the system model. Relaxation of this assumption, allowing thus the investigation of asymmetric couplings as well, is possible through the use of generating functional techniques. The results obtained for the asymmetric interactions, however, are qualitatively similar to those for the symmetric case [10].

The main finding of the study of the model ecosystem defined by equations (1) and (6) is that ecosystems characterized by predominantly cooperative interspecies interactions ($\beta' > 0$) exhibit very low diversity, as opposed to those for which the competition prevails. Then it follows the somewhat peculiar conclusion that the interspecies competition promotes species diversity.

Acknowledgments

The work of JFF was supported in part by Conselho Nacional de Desenvolvimento CientÍfico e Tecnológico and Fundação de Amparo à Pesquisa do Estado de São Paulo (FAPESP), project no 04/06156-3. FCP was supported by FAPESP.

References

[1] Mézard M, Parisi G and Virasoro M A 1987 *Spin Glass Theory and Beyond* (Singapore: World Scientific)
[2] Fischer K H and Hertz J A 1991 *Spin Glasses* (Cambridge: Cambridge University Press)
[3] Ridley M 1996 *Evolution* (Cambridge: Blackwell)
[4] Coolen A C C, Penney R W and Sherrington D 1993 *Phys. Rev.* B **48** 16116
[5] Penney R W, Coolen A C C and Sherrington D 1993 *J. Phys. A: Math. Gen.* **26** 3681
[6] Dotsenko V, Franz S and Mézard M 1994 *J. Phys. A: Math. Gen.* **27** 2351
[7] Diederich S and Opper M 1989 *Phys. Rev.* A **39** 4333
[8] Biscari P and Parisi G 1995 *J. Phys. A: Math. Gen.* **28** 4697
[9] de Oliveira V M and Fontanari J F 2000 *Phys. Rev. Lett.* **85** 4984
de Oliveira V M and Fontanari J F 2001 *Phys. Rev.* E **64** 051911
de Oliveira V M and Fontanari J F 2002 *Phys. Rev. Lett.* **89** 148101
[10] Galla T 2005 *J. Stat. Mech.* P11005
Galla T 2006 *J. Phys. A: Math. Gen.* **39** 3853
[11] Poderoso F C and Fontanari J F 2005 *Eur. Phys. J.* B **48** 557
Poderoso F C and Fontanari J F 2006 *Phys. Rev.* E **74** 051919
[12] Schuster P and Sigmund K 1983 *J. Theor. Biol.* **100** 533
[13] Hofbauer J and Sigmund K 1998 *Evolutionary Games and Population Dynamics* (Cambridge: Cambridge University Press)
[14] Amit D J 1989 *Modeling Brain Function: The World of Attractor Neural Networks* (Cambridge: Cambridge University Press)
[15] van Hemmen J L and Palmer R G 1979 *J. Phys. A: Math. Gen.* **12** 563
[16] Simpson E H 1949 *Nature (London)* **163** 688

[17] Rényi A 1961 *Proc. 4th Berkeley Symp. Math. Stat. and Probability* vol 1 (Berkeley: University of California Press) pp 547–61
[18] de Almeida J R L and Thouless D J 1978 *J. Phys. A: Math. Gen.* **11** 983
[19] Nogueira E and Fontanari J F 2003 *Physica* A **329** 365
[20] Fisher R A, Corbet A S and Williams C 1943 *J. Anim. Ecol.* **12** 42
[21] Hairston N G 1959 *Ecology* **40** 404
[22] Nee S, Harvey P H and May R M 1991 *Proc. R. Soc.* B **243** 161
[23] Szabó G and Czárán T 2001 *Phys. Rev.* E **63** 061904
[24] Szabó G 2005 *J. Phys. A: Math. Gen.* **38** 6689